Nanobalance: the European balance for micro-propulsion

IEPC-2009-182

Presented at the 31st International Electric Propulsion Conference,
University of Michigan • Ann Arbor, Michigan • USA
September 20 – 24, 2009

Stefano Cesare, Fabio Musso, Filippo D'Angelo, Giuseppe Castorina
Thales Alenia Space Italia, Strada Antica di Collegno 253, 10146 Turin, Italy

Marco Bisi, Paolo Cordiale
Istituto Nazionale di Ricerca Metrologica, Strada delle Cacce 73, 10135 Turin, Italy

Enrico Canuto
Politecnico di Torino, Corso Duca degli Abruzzi 24, 10129 Turin, Italy

Davide Nicolini, Eliseo Balaguer, Pierre-Etienne Frigot
ESA-ESTEC, Keplerlaan 1, 2201 AZ Noordwijk ZH, The Netherlands

Abstract: Within a contract of the European Space Agency, Thales Alenia Space Italia in co-operation with the Italian National Metrology Institute and Polytechnic of Turin, has designed and implemented the Nanobalance Facility, a device for the direct measurements of the force of micro-thrusters (of electrical and cold-gas type).
The Nanobalance is aimed to support the development of micro-propulsion technologies for major European space programs as LISA-Pathfinder, Microscope and GAIA.
The Nanobalance thrust stand is essentially composed by two vertical "tilting plates" connected by a flexible joint to a rigid block made of Zerodur®, in a pendulum-like arrangement. The micro-thruster to be characterized is installed on one of the tilting plates. A counterweight is installed on the second tilting plate to ensure the same dynamics behavior of the first one and therefore the rejection of the common-mode environmental vibrations acting on the thrust stand.
When the micro-thruster is switched on, it produces a displacement of one plate relative to the other, which is measured by means of a Fabry-Perot laser interferometer, which reference spherical mirrors are mounted on the tilting plates. The Fabry-Perot interferometer is fed by an Nd:YAG source working at the wavelength λ = 532 nm (2nd harmonic). The laser frequency is regulated so as to maintain it locked to the F-P resonator as the relative distance between the two mirrors changes under the action of the MT (the laser frequency tracks the distance variation).
The frequency of this laser (measurement laser) is measured against the frequency on an identical Nd:YAG laser (reference laser) stabilized on a Iodine molecular transition using the Pound-Drever technique. This frequency measurement is converted in a force measurement using a calibration relationship, verified by means of a voice coil actuator permanently installed on the tilting plate and operable even during the test campaign on the micro-thruster.
The Nanobalance thrust stand is operated inside a vacuum chamber capable to maintain the pressure below $1 \cdot e^{-4}$ mBar while a cold-gas thruster is firing, and below $1e^{-6}$ mBar while an electrical thruster is firing. Inside the chamber, the thrust stand is mounted on a horizontal basement which inclination is actively controlled to zero. The vacuum chamber is installed on six pneumatic isolators, rested on an anti-seismic block.
The Nanobalance has been fully commissioned without thruster and with representative thrusters (pressurized micro-valve and ion source): it has a force resolution = 0.1 μN and an intrinsic force measurement noise spectral density $\leq 0.1\ \mu N/Hz^{1/2}$ between 0.01 and 1 Hz ($\leq 1\ \mu N/Hz^{1/2}$ down to 1 mHz), over a measurement range of 1 mN. The Nanobalance has been already utilized for test campaigns on a cold-gas thruster and on an electrical thruster (FEEP type).

Nomenclature

c	=	speed of light in vacuum.
f	=	pendulum natural frequency
FPI	=	Fabry-Perot Interferometer
F_t	=	thrust force
K	=	joint stiffness
MT	=	micro-thruster
ν_l	=	light frequency
λ_l	=	light frequency

I. Introduction

FUTURE space missions, like LISA Path Finder, GAIA, and MICROSCOPE, rely on low noise microthrusters for achieving the spacecraft attitude and orbit control requirements. In particular 'drag-free' space missions like LISA and its precursor LISA Pathfinder rely on low noise micro-thrusters for keeping their flight free-falling, hence sensitive to extremely low gravity-field perturbations. Micro-thrusters have to deliver continuous thrust ranging from 0.1 μN to 1 mN with a noise level better than 0.1 μN/ √Hz in a frequency band from 0.1 mHz to 2 Hz . Thrust-stands for measuring thrust and noise lower than micro-Newton accuracy are under test in Europe and United States. The Nanobalance instrument has been conceived around an in-vacuum Fabry-Pérot cavity made by two highly reflective mirrors mounted on the bottom of two parallel metallic plates, the active and passive pendulum, which are suspended to an athermic spacer by means of flexible joints (see Figure 1). The thruster under test is mounted on the active pendulum and balanced by a dummy one on the passive pendulum. Under perfectly equal pendulums and zero thrust the Nanobalance would reach equilibrium and the cavity length would be kept constant although both pendulums were oscillating subjected to ground noise.

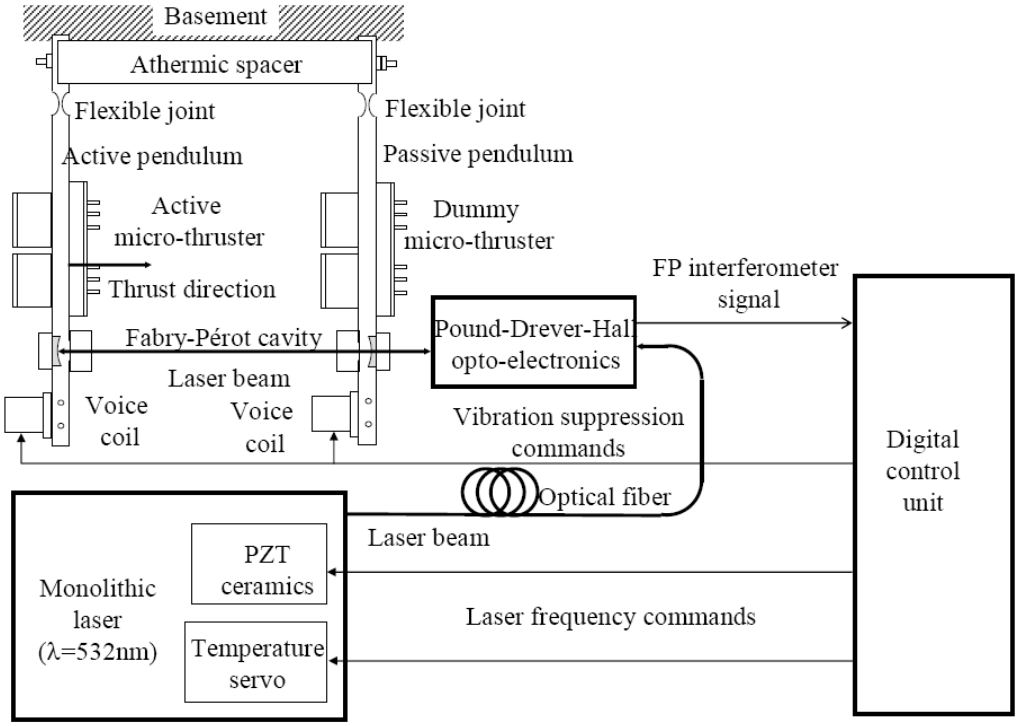

Figure 1, Sketch and block diagram of the instrument.

By driving the frequency of the injected laser beam to keep the cavity close to a resonant condition under variable length, the tunable frequency becomes proportional to cavity length deviations and therefore to the actuated thrust. This is achieved by servoing the built-in frequency actuators of the laser source to the interferometer output signal. By 'beating' the incident laser beam with a stabilized laser source, the tunable frequency can be accurately recorded and the actuated thrust measured.

II. Instrument principle

The fundamental instrument equations

The force balance (see Figure 1) is made by two Cu-Be plates, the pendulums, which should be equal in geometry and mass distribution. Their upper pivots, made by flexible joints, are kept at constant distance by an athermic spacer: a Zerodur® plate having a very low coefficient of thermal expansion, below 0.1×10^{-6} K^{-1}. The micro-thruster (MT) under test is mounted on the active pendulum, the left one in Figure 1. To balance the active micro-thruster, a dummy one is mounted on the passive pendulum, the right one in Figure 1. A voice coil is mounted on the bottom of each pendulum. Joint stiffness K and pendulum geometry and mass have been designed to provide each pendulum with a natural frequency $f_j \geq 10$ Hz. By applying the thrust F_t at a distance L_t from the joint axis and by measuring the pendulum displacement ΔL at a distance L_m from the same axis, the displacement-to-thrust scale factor $K_{\Delta L}$ results:

$$F_t = \frac{K}{L_m \cdot L_t} \cdot \Delta L = K_{\Delta L} \cdot \Delta L \qquad (1)$$

showing need of a sub-nanometric displacement sensor.
Distance variations between pendulums are revealed by a Fabry-Pérot optical cavity, which consists of two highly-reflecting mirrors mounted on the lower part of each plate.
The visible radiation of a frequency-duplicated monolithic laser is injected into the mirror cavity from one side. The monolithic laser medium is a ring oscillator made by a Nd-doped YAG crystal (Yttrium-Aluminum Garnet) which is optically pumped by a laser diode to emit a coherent light-wave in the near infrared (λ_{YAG} = 1064 nm). The emitted light is then frequency–duplicated to provide a visible beam with a frequency ν_l tunable around $\nu_0 = 2c/\lambda_{YAG}$ ≈ 564 THz.
When the Nanobalance cavity length L , defined as the mean light path between the mirror optical centers, is made proportional to a multiple N of the half wavelength $0.5\lambda_l = 0.5c/\nu_l$ of the incident light-wave, the resonant condition establishes

$$L = N \cdot \lambda_l/2 \Rightarrow \nu_l = N \cdot c/2 \ , \qquad N \text{ integer} \qquad (2)$$

c being the speed of light in vacuum. A pair $(\nu_l \ , \ L)$ satisfying (2) is called a resonant pair, and is denoted as $(\nu_0(N), L_0(N))$.
The frequency distance

$$FSR_0 = c/\ (2L_0) \qquad (3)$$

between two resonant pairs is the so called *Free Spectral Range*, where L_0 is the FPI cavity length.

Actually condition (2) can not be exactly met but only approached, by forcing frequency and length to fluctuate around a resonant pair through active control. Thus by denoting length detuning with $\Delta L = L - L_0(N)$ and

frequency detuning with $\Delta\nu = \nu_l - \nu_0(N)$, a linear differential equation relating length and frequency to the cavity detuning e can be written as

$$\Delta\nu + k_0 \Delta L = e \quad , \qquad k_0 = \nu_0 / L_0(N) \tag{4}$$

The above relation, called lock-in condition, is the fundamental instrument equation and holds for a detuning e which is sufficiently small with respect to the cavity Free Spectral Range.
The current Nanobalance shows a typical k_0 value around 2.9 MHz/nm.

III. Facility architecture

The Nanobalance Facility architecture is schematized in Figure 1.3-1 and consists of the following elements:

- **Thrust Stand:** It consists of two tilting plates made in Copper Beryllium alloy, each connected by an elastic joint to a rigid spacer made of Zerodur®. The natural frequency of the tilting plates is 13.44 Hz, without MT installed.

  The MT to be characterized is installed on one of the tilting plates. A second, passive, MT (or a dummy MT) is installed on the second tilting plate for balancing purpose (the natural oscillation frequency of the two tilting plates shall be made as much identical as possible).

- **Vacuum System**. It consists of a cylindrical vacuum chamber (internal length = 2.5 m, internal diameter = 1.2 m) and a vacuum pump group comprising one primary pump (Leybold Scroll SC 30 D with nominal pumping speed = 30 m^3/hr), one turbomolecular pump (Leybold MAG W 2200 with nominal pumping speed of N_2 = 1600 l/s), two ion pumps (Varian VacIon 500 with nominal pumping speed of N_2 = 410 l/s).

  The vacuum chamber frame rests on four pneumatic isolators. The chamber has two large doors and can be split in two parts for a full access to the Thrust Stand.

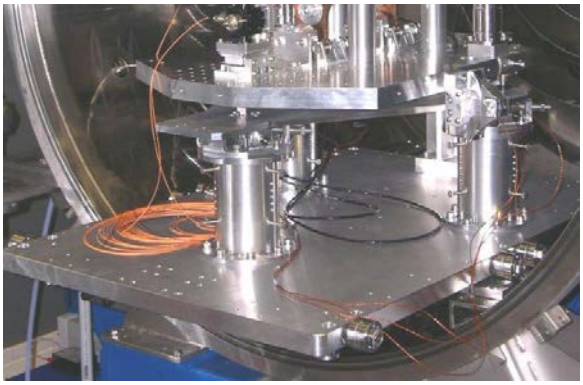

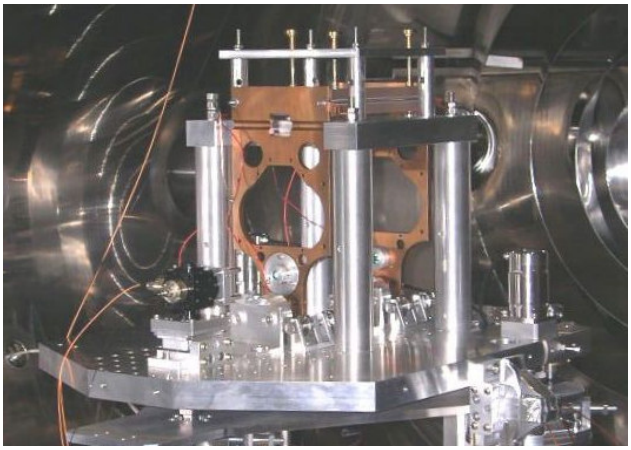

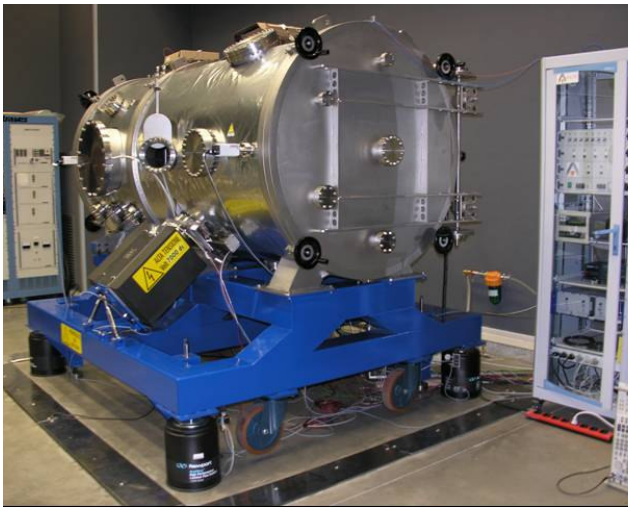

- **Horizontality Control Stage**. It is a device interposed between the Thrust Stand base plate and the vacuum chamber. Its function is to keep the Thrust Stand horizontality operating by means of two piezoelectric motors driven by the measurement of a tiltmeter installed on top of the Zerodur® spacer. This stage includes also a passive decoupling system for further reducing the horizontal accelerations at the NB Thrust Stand along the measurement direction.

- **Metrology System**. It consists of a Fabry-Perot laser interferometer and of an opto-mechanical setup by means of which the relative displacement of the tilting plates produced by the micro-thruster force is measured.

  The metrology system is fed by two Nd:YAG lasers (Innolight Prometheus 20), one of which is frequency stabilized on a Iodine cell. The micro-thruster force information is derived from the beat frequency of these two lasers (reference laser, measurement laser), which is measured by a frequency-meter.

- **Monitoring and Control System**. It includes the workstations and I/O devices in charge of controlling the Horizontality Control Stage and the Metrology System, of monitoring the pressure of the vacuum chamber, the temperatures and inclination of the Thrust Stand. It acquires the output of the frequency-meter and converting it in real time into the force measurement. It includes also a Graphic User Interface (GUI) for controlling the NB parameters and for real-time display of the measured force.

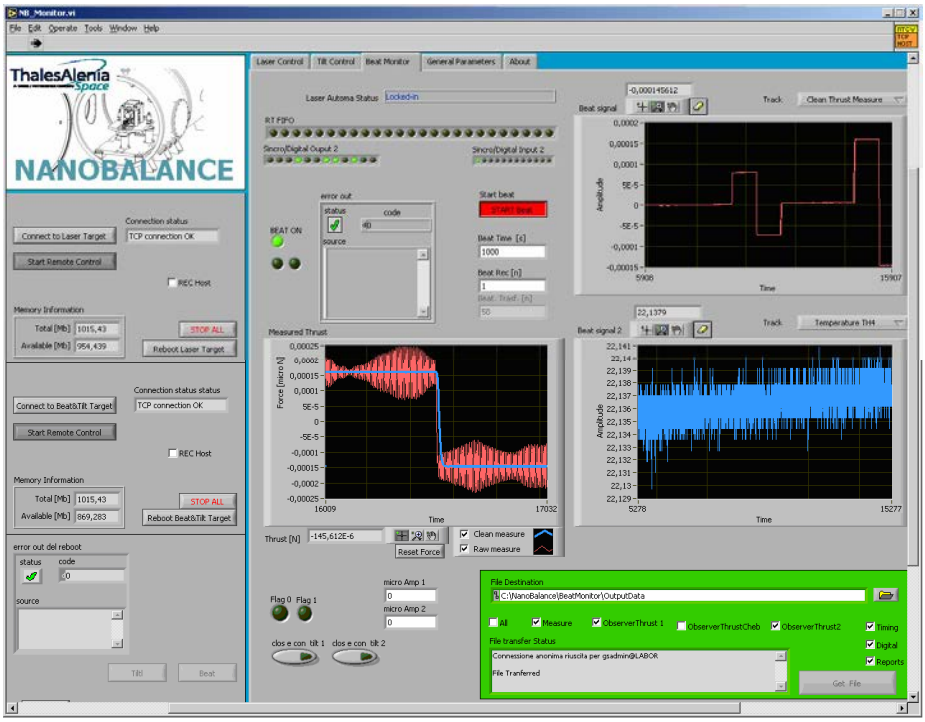

Figure 2, NB Monitoring and Control System: Graphic User Interface

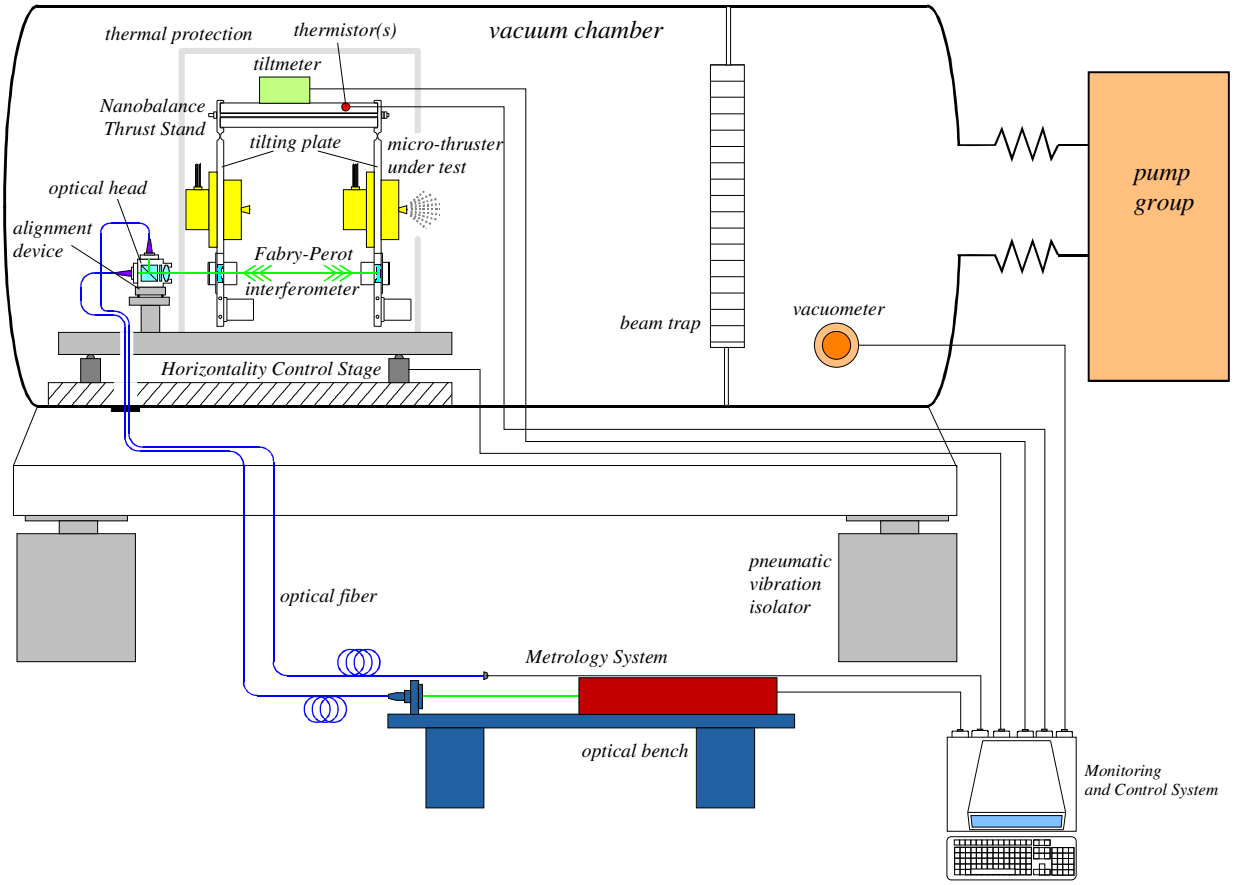

Figure 3, General architecture of the Nanobalance Facility

IV. Measurements and performances

A. Measurement of the Micro-Thruster Force

The force (F_T) produced by the micro-thruster induces a distance variation (δl) between the optical references installed on the tilting plates of the NB Thrust Stand. This displacement is detected by the laser interferometer: in particular a displacement (δl) corresponds to a frequency variation ($\delta \nu_L$) of the measurement laser frequency (ν_L), counted by the frequency-meter of the Metrology System from the instant in which the thruster has started firing. The frequency variation is measured by the frequency-meter (sampled at 1 kHz) and recorded by the Monitoring and Control System versus time at a 100 Hz rate after an average performed on consecutive sets of 10 measurements each to remove the aliasing effect of the high frequency disturbances: this time history of the laser frequency variation is the raw measurement of the NB.

The relationship between the displacement (δl) and the frequency variation ($\delta \nu_L$) is linear. The relationship between the force (F_T) and the displacement (δl) is also linear within the whole measurement range of the NB and for force variations frequencies ~10 times smaller than the resonance frequency of the tilting plate (around 12 Hz

with the MT installed). The frequency variation ($\delta\nu_L$) is then transformed into a force $\hat{F}''$ applied perpendicularly to the tilting plate in the point where the micro-thruster (MT) is mounted through the following linear relationship:

$$\hat{F}'' = K_{NB}\delta\nu_L$$

where the constant K_{NB} is the Nanobalance scale factor, depending on the position of the force application point and on the stiffness of the suspension of the tilting plate when the MT is installed (i.e. including the effect of the cabling and piping). The linearity of the above relationship is shown in Figure 4. The time history of $\hat{F}''$ is the raw force measurement of the NB.

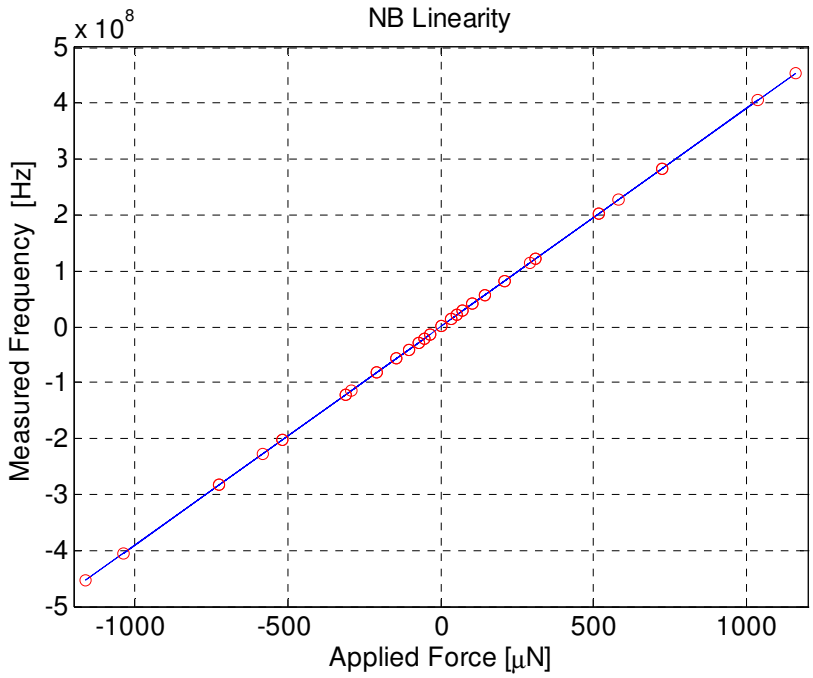

Figure 4, Plot showing the linear relationship between different values of known forces (F_T) applied to the NB Thrust Stand and measured frequency variations ($\delta\nu_L$), extended up to ~ ±1 mN forces.

The force $\hat{F}''$ is passed, in parallel, through a pair of in-line low-pass filters:

1) a wide-band state predictor (6th order), tuned on the natural vibrations of the tilting plates, which cuts the harmonic components above ~4÷5 Hz, while preserving a response time < 150 ms;
2) a narrow-band state predictor (4th order), tuned on the worst-case NB basement vibration inside the measurement band (around 0.7 Hz), for further smoothing the raw measurements at the cost of a longer response time (> 1 s).

The response comparison of the two filters to a force step of 50 μN applied to the NB is shown in Figure 5.

The quantities $\hat{F}'$ (output of wide-band filter) and $\hat{F}'_{nb}$ (output of narrow-band filter) represent the real-time force measurements provided by the NB. They give a first estimate of the force (F_T) produced by the MT. The discrepancy is due to the fact that other physical phenomena (thermo-elastic deformations of the Thrust Stand, variations of the Thrust Stand inclination, pressure variations inside the vacuum chamber) other that the MT action can produce a displacements (δl). The effects of these physical phenomena on the force measurement are estimated

(in the post processing) from the temperature of the Thrust Stand, the inclination of the Thrust Stand and the pressure inside the vacuum chamber, which are measured in parallel to the force. Then, these effects are subtracted from the real-time force measurement to obtain (after the post processing) the force $\hat{F}$ which represents the best estimate of the force (F_T) produced by the MT. An example of force measurement processing is given in Chapter V.

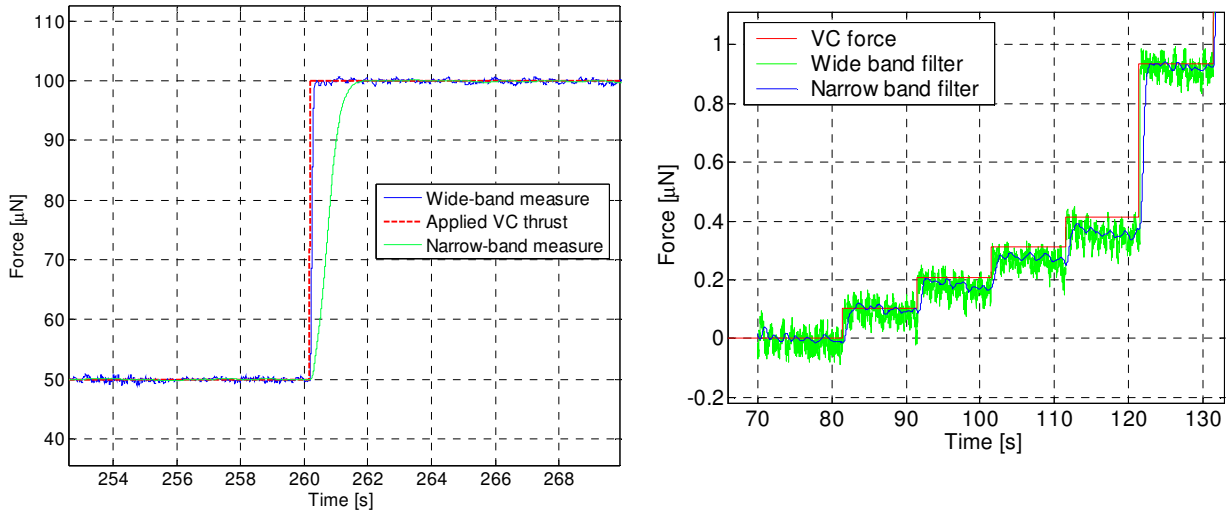

Figure 5, (Left): Wide-band and narrow-band filters response to 50 μN force step. (Right): Measurement resolution

B. Determination of the Nanobalance Scale Factor

The NB scale factor is determined before just starting any test campaign (with the MT installed and the Thrust Stand under vacuum) using a voice coil installed in the lower part of the same tilting plate of the MT (see Figure 6) and calibrated against a second voice coil previously calibrated at the Italian Metrological Institute INRIM.

The method consists in applying with the voice coil a sequence of three force step pairs (each pair is composed by two consecutive steps of equal amplitude and opposite sign) of known and increasing amplitude (F_{VC}) of 35 μN, 70 μN, 140 μN, 280 μN (equivalent force in an application point placed 10 cm below the tilting plate hinge, i.e., in proximity of the MT position). The laser frequency variation ($\delta\nu_L$) is measured in correspondence of each force step. The angular coefficient of the straight line fitting the (F_{VC}, $\delta\nu_L$) points is the NB scale factor at the voice coil location ($K_{NB\text{-}VC}$, μN/MHz), i.e. this scale factor translate a frequency variation into a force applied to the tilting plate in the point where the voice coil is mounted. From $K_{NB\text{-}VC}$, the NB scale factor K_{NB} (transforming the frequency variation ($\delta\nu_L$) into the force applied perpendicularly to the tilting plate in the point where the MT is mounted) is then computed as follows:

$$K_{NB} = \frac{L_V}{L_T} K_{NB-VC}$$

where:

- L_T is the distance from the hinge of the tilting plate to the application point of the micro-thruster force;
- L_V is the distance from the hinge of the tilting plate to the application point of the voice coil force.

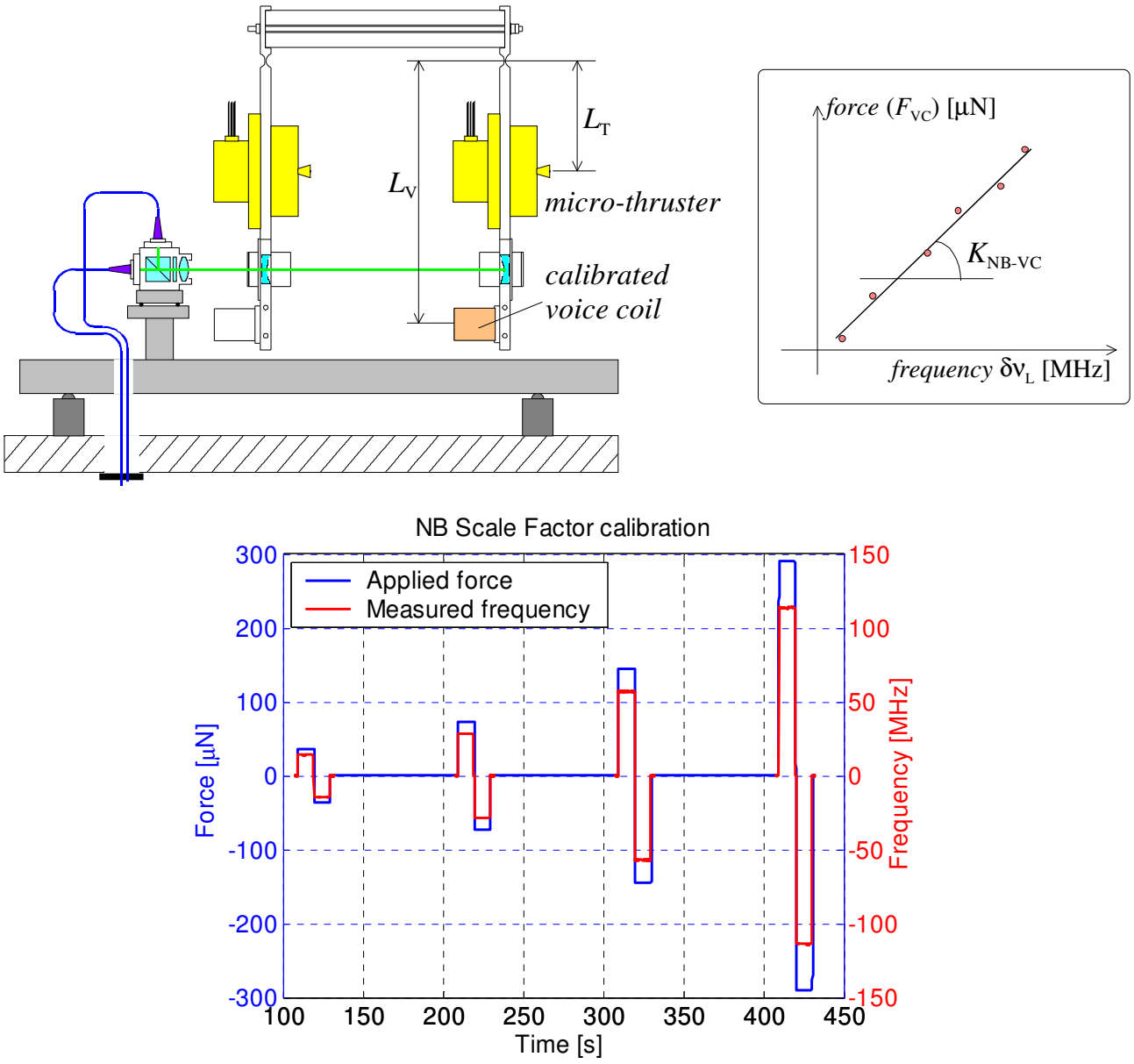

Figure 6, Calibration of NB scale factor using the calibrated voice coil.

The distances L_V, L_T are measured by means of a photogrammetry technique (using a telecentric objective) after the installation of the MT on the tilting plate and before closing the vacuum chamber. The MT manufacturer shall indicate the precise location of the force application point with respect to the MT features observable in the pictures, like for instance the nozzle.

Indicatively, the scale factor of the NB is:

$$K_{NB} \cong 2.5\ \mu N/MHz$$

The actual value of the scale factor depends on the MT installed on the tilting plate and is determined by calibration before any test campaign.

The apparatus used for the photogrammetry is shown in Figure 7.

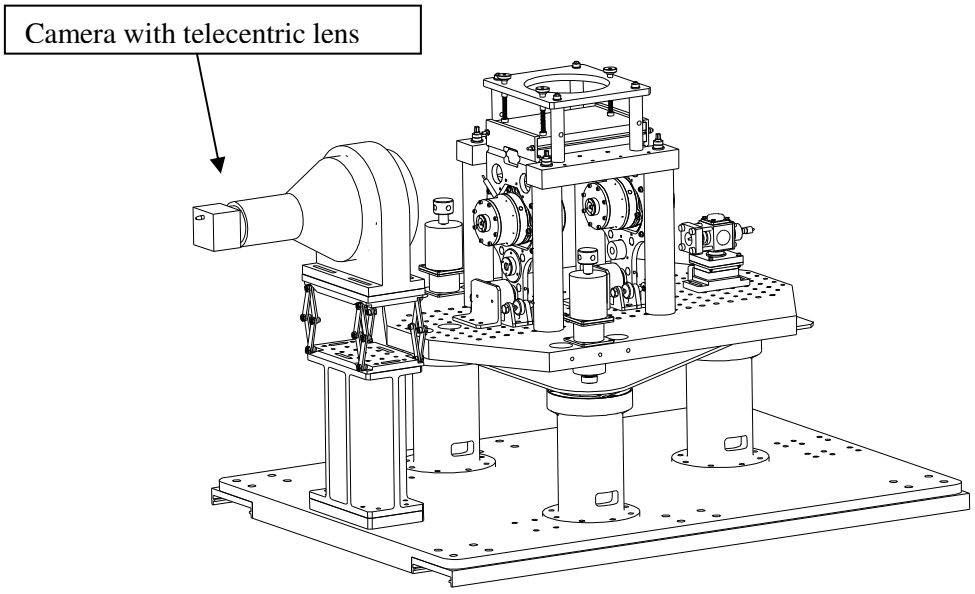

Figure 7, Photogrammetry apparatus used to determine the micro-thruster and voice coil position relative to the hinge of the tilting plate.

C. Measurable Micro-Thruster parameters and measurement performances

The following Table 1 provides the list of the micro-thruster parameters measurable by the Nanobalance and the corresponding measurement performances, after post processing. These performances are characteristics of the Nanobalance alone, and have been determined without micro-thrusters installed on it. The operation of the micro-thruster can induce reactions on the Nanobalance (pressure increase and drag forces on the tilting plates due to the gas injected in the vacuum chamber, electrostatic forces due to high voltages, thermo-elastic deformations of the Thrust Stand due to micro-thruster thermal dissipation, variation of the tilting plate CoM position due to thruster valve motion, etc..) that may change the performance figures, and in particular the accuracy. These effects cannot be neglected, and must be assessed case by case by proper sensitivity tests on the micro-thruster before starting the test campaign. The results of these characterization tests will enable to determine the performances (and in particular the measurement accuracy) guaranteed by the Nanobalance for the tests on that specific micro-thruster.

Measured parameter	Measurement performance
Thrust range	up to 1 mN
Thrust resolution	0.1 μN
Thrust accuracy (see Annex B for a detailed accuracy budget)	$T_{measured} = T_{actual} \pm (0.65\ \mu N + 1\% \cdot T_{actual})$
Thrust Slew rate	up to 1.5 μN/ms
Thrust Rise/fall time	The NB is capable to attain up to 90% of a 36 μN commanded force step in 100 ms.
Thrust noise	$< 0.1\ \mu N/\sqrt{Hz}$ from 1 to 0.01 Hz $\leq 0.1 \times \frac{0.01}{f}\ \mu N/\sqrt{Hz}$ for $f < 0.01$ Hz

Table 1, Micro-Thruster measurable parameters and Nanobalance performances

V. Force measurement processing methodology

A. Real Time Processing

The raw measurement of the NB consist in the time history of the frequency variation of the measurement laser ($\delta\nu_L$, Hz) measured by the frequency-meter, sampled at 1 kHz (1 ms time step) and recorded by the Monitoring and Control System at a 100 Hz rate (10 ms time step) after an average performed on consecutive sets of 10 measurements each to remove the aliasing effect of the high frequency disturbances. An example of this raw measurement is shown in Figure 8.

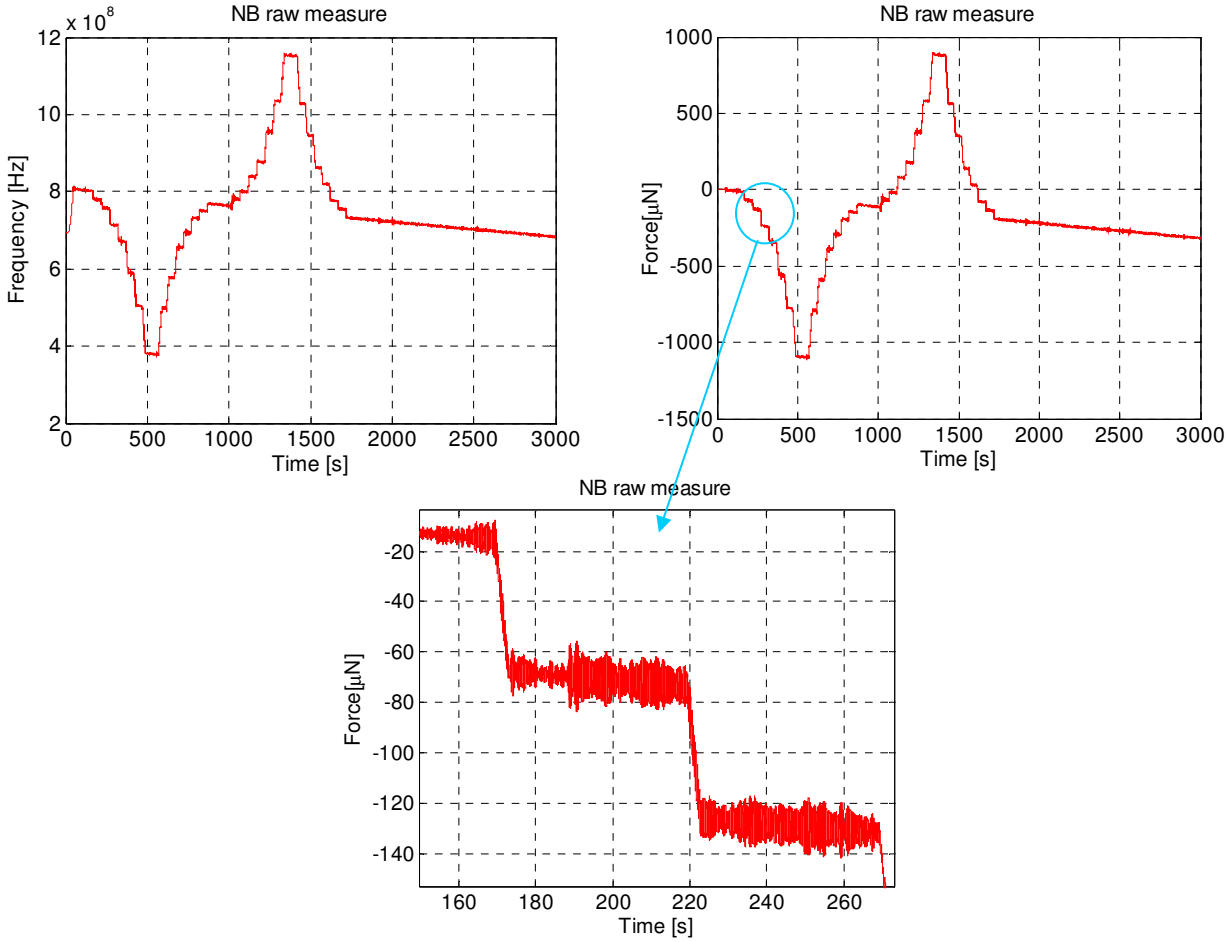

Figure 8, (Top left): Time history of the frequency variation (δνL). (Top right): Time history of the force $\hat{F}'' = K_{NB}\,\delta\nu_L$. (Bottom) Magnification of a portion of $\hat{F}''$ showing the high-frequency oscillations superimposed to the force profile and mainly due to the natural frequencies of the tilting plates.

The first operation performed on this raw measurement is to convert it in force ($\hat{F}''$, N) by multiplying $\delta\nu_L$ by the K_{NB} is the Nanobalance scale factor measured before the micro-thruster test using the calibrated voice coil permanently installed on the tilting plate. This force directly obtained from the frequency conversion is shown in Figure 8.

The force bias present when the measurements are started is computed on $\hat{F}''$ by taking its average value over the first 5 s, and zeroed. The NB then measures force variations from this initial zero value.

This time history is then passed through the two real-time low-pass filters (narrow-band, wide-band). The time histories of the forces $\hat{F}'_{nb}$ (output of narrow-band filter) and $\hat{F}'$ (output of wide-band filter) obtained from the previous $\hat{F}''$ are shown in Figure 9. The high frequencies (and in particular the tilting plate natural frequencies) are now filtered out, and the profile of the force applied is only affected by the noise with spectral contents below the cut-off frequency of the filters (~4÷5 Hz for the wide-band filter, ~0.7 Hz for the narrow-band filter) and by a drift.

The frequency variation and all the forces $\hat{F}''$, $\hat{F}'$, $\hat{F}'_{nb}$ are displayed in real time on the screen of the Monitor and Control System.

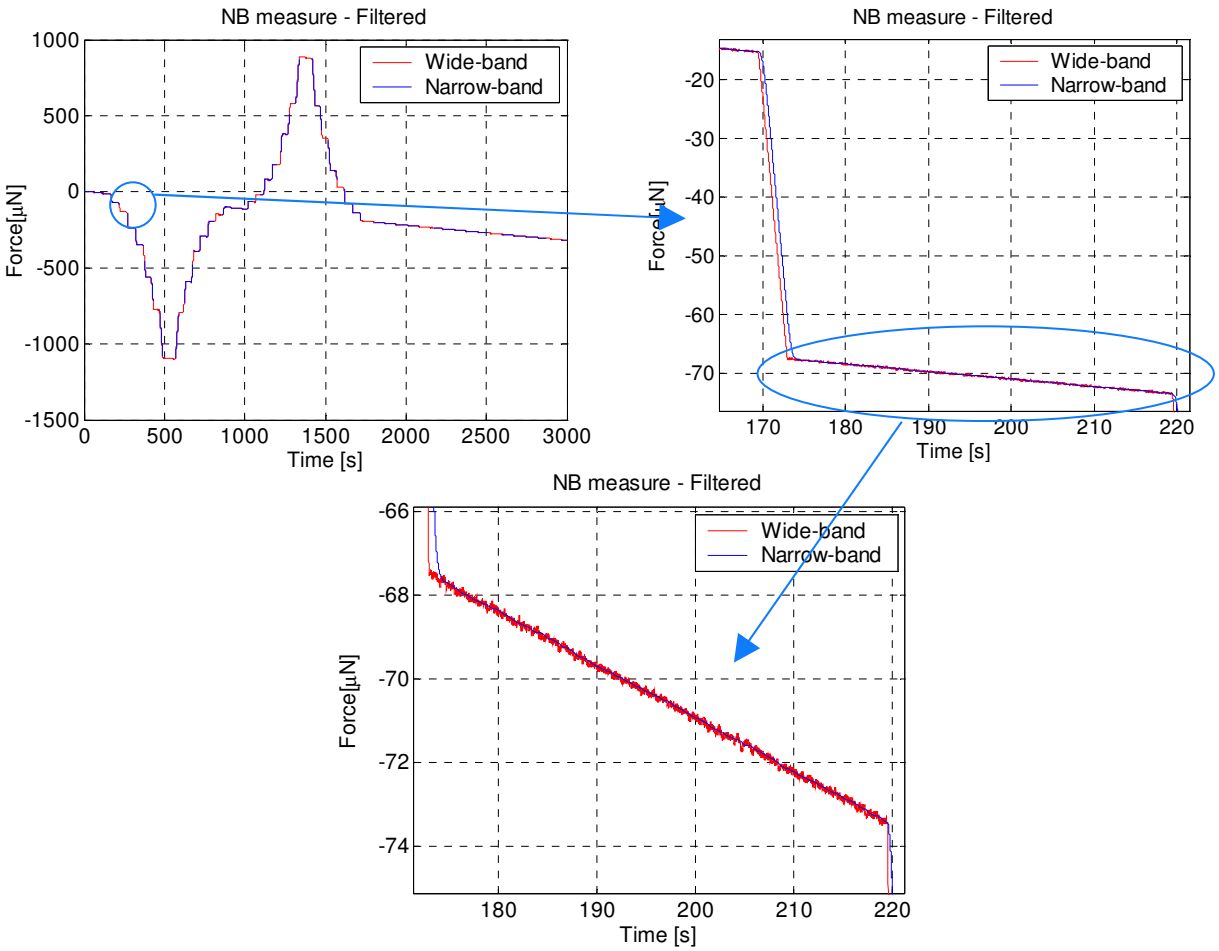

Figure 9, (Top left): Time histories of the forces $\hat{F}'_{nb}$ (output of narrow-band filter) and $\hat{F}'$ (output of wide-band filter). (Top right): Magnification the first portion of $\hat{F}'_{nb}, \hat{F}'$. (Bottom): Further magnification a portion of $\hat{F}'_{nb}, \hat{F}'$ showing the difference between the two force profiles due to the different shape of the two low-pass filters.

B. Micro-Thruster Independent Post-Processing and Drift Removal

The force $\hat{F}'$ (output of wide-band filter) is processed to remove the drift. This drift has been found to be correlated with the temperatures of the Thrust Stand which is measured in several locations by a set of thermistors. The temperature of Zerodur® spacer is one showing the highest degree of correlation with the temperature.

The procedure for the drift removal consists in fitting the temperature profile with polynomial of increasing degrees (1^{st} = straight line, 2^{nd} = parabola, 3^{rd} = cubic, …) and looking at the residuals after having subtracted the polynomial fit. This procedure is stopped when the residual has the characteristics of a random noise without deterministic behaviors: this established the highest degree of the polynomial representing the temperature drift. Then, the time history of the force $\hat{F}'$ is fitted with a polynomial of the same degree (in the zones where the command is not applied) and the polynomial fit so obtained is subtracted from $\hat{F}'$ to get the drift-free force estimate $\hat{F}$.

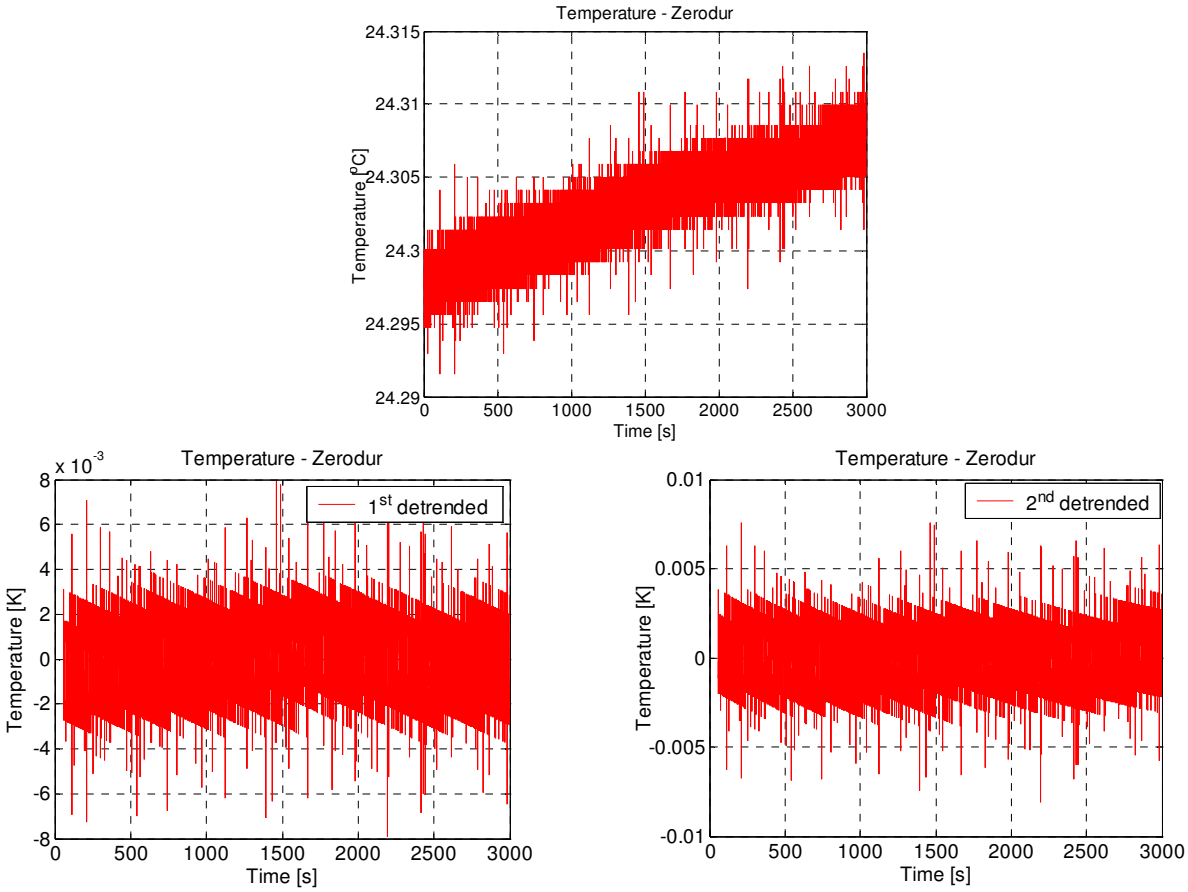

Figure 10, (Top): Time history of the temperature of the Zerodur® spacer recorded during the measurement of the force profile $\hat{F}'$. (Bottom left): Residual of the temperature after the subtraction of a 1^{st} order polynomial fit: a slight deterministic behavior is still present. (Bottom right): Residual of the temperature after the subtraction of a 2^{nd} order polynomial fit: the behavior has now a total randomic nature. Note: due to the very small temperature variation, the noise is dominated by the measurement quantization.

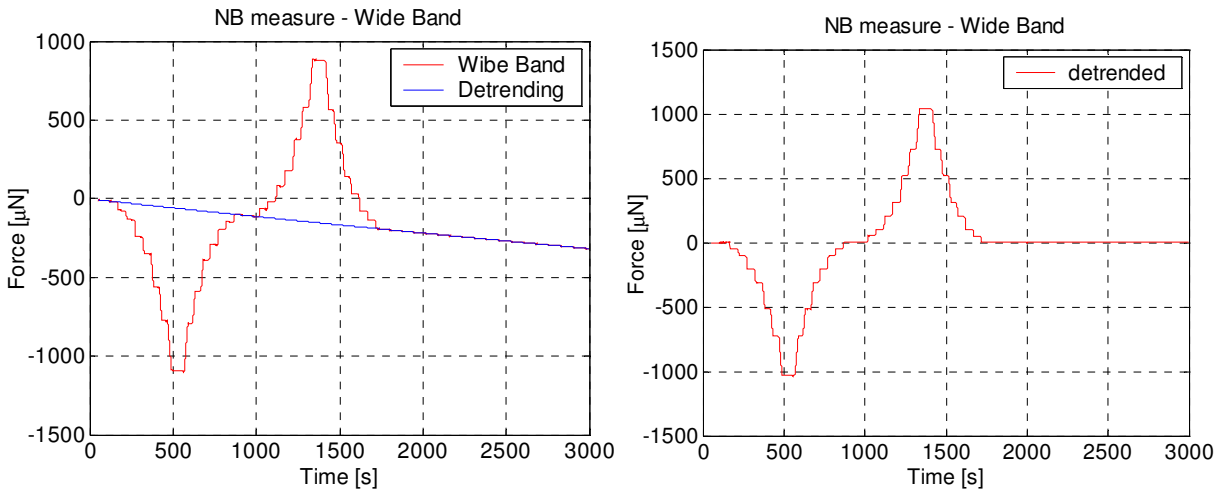

Figure 11, (Left): Time history of the force $\hat{F}'$ and of the 2nd order polynomial fit estimating its drift (blue line). (Right): Time history of the force $\hat{F}$ ($\hat{F}'$ after the subtraction the 2nd order polynomial fit).

C. Micro-Thruster Dependent Post-Processing

After the trend removal, a further processing of the MT force is applied on a case by case basis to remove the possible spurious forces caused by the MT operation (e.g. the effect of the pressure increase and drag on the tilting plates due to the gas injected in the chamber, or the electrostatic forces due to the applied high voltages, or the variation of the tilting plate CoM position due to thruster valve motion). This spurious force removal is based on a model defined during a characterization phase, before starting the test campaign, and correlating the spurious force to a parameter linked to cause of the spurious force and measurable during the tests (e.g. the gas flow, the pressure inside the vacuum camber, the voltage applied to the thruster).

VI. Error Budget and Thrust Accuracy

The thrust measurement accuracy is determined by the residual force measurement noise after the post-processing (that defines the constant part of the measurement error) and by the error in the determination of the NB scale factor (that defines the part of the error proportional to the input force).

1) The force measurement noise of the NB has been derived from a long-duration test during which no force has been applied to the Thrust Stand through an actuator. The raw measurements have been prost-processed for subtracting deterministic components due to thermal effects, expressed as a n^{th} order polynomial, with $n \leq 3$. The resulting residual force measurement noise in time and frequency domain is shown in Figure 12. Note the 1st order random drift below 0.01 Hz, still to be investigated. To be conservative, the constant part of the measurement error has been estimated from the long-term standard deviation of the random drift mean profile shown in Figure 12 (dashed line). By defining long term as $t_0 = 10000\ s$, the drift standard deviation $s(t_0)$ amounts to

$$s(t_0) = 0.0065\ (t_0)^{1/2} = 0.65\ \mu\text{N}$$

The resulting value should be compared to the RMS of the time profile in Figure 12, left, close to 0.1 μN. Only a slight contingency factor equal to 1.5 has been included as the drift variance is rather conservative, since any random drift realization may be cleaned from its mean value.

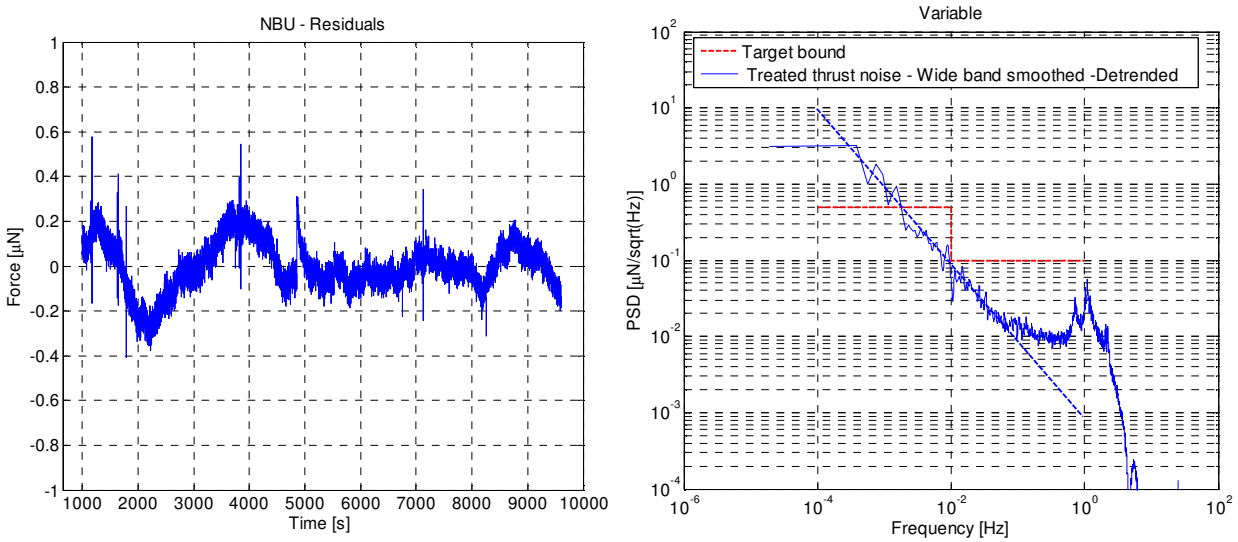

Figure 12, Residual force measurement noise of the NB. (Left): time profile. (Right): spectral density. The right plot shows the low-frequency drift model (dashed line) used to estimate the constant part of the measurement error.

2) The error budget in the determination of the NB scale factor (K_{NB}) is provided in Table 2. The resulting total fractional error is 0.01 (1%). Therefore the resulting thrust measurement accuracy is:

$$F_{\text{measured}} = F_{\text{actual}} \pm (0.65\ \mu\text{N} + 1\% \cdot T_{\text{actual}})$$

This accuracy doesn't take into account measurement errors that may be originated by the gas plume impingement on the Thrust Stand, pressure variations inside the feeding pipe, voltage variations in the micro-thruster cables and moving parts inside the micro-thrusters, as these effects are specifically functions of the micro-thruster under tests and must be characterized on a case-by-case basis.

Quantity	Unit	Typical Value	Uncertainty upper bound [fraction]	Comments
VC thrust constant	μN/div	0.104	0.007	From the calibration of the VC permanently installed on the tilting plate with the calibrated VC
VC scale factor	MHz/div	0.0883	0.001	From the VC scale factor estimation algorithm
MT lever arm/VC lever arm ratio		0.465	0.002	From the accuracy achievable by photogrammetry
Total			0.01	

Table 2, Error budget affecting the determination of the NB scale factor

The uncertainty of the VC thrust constant (1st row in Table 2) has been obtained by calibrating the VC permanently installed on the tilting plate (lower voice coil) against another voice coil previously calibrated at INRIM mounted on the same tilting plate in the upper position (upper voice coil).

VII. Nanobalance performance in representative test bed

After NB characterization tests performed with voice coils, further measurements have been performed with real thrusters: a cold-gas thruster (CGT) fed by Nitrogen and an electrical FEEP thruster fed by Indium. These tests have been made as a last commissioning step, in order to demonstrate the performance in a representative test bed, in preparation of future Micro-Thruster test campaigns.
The purpose was to investigate the impacts on the NB force measurement due to the test set-up and to the thruster operation, in order to eliminate such effects by post-processing. These are represented by the parasitic noise effect listed in the followings:

A. FEEP thrusters

The following effects have been investigated:

- background noise and parasitic force effect due to high voltage (to be zeroed before FEEP firing) , Figure 13

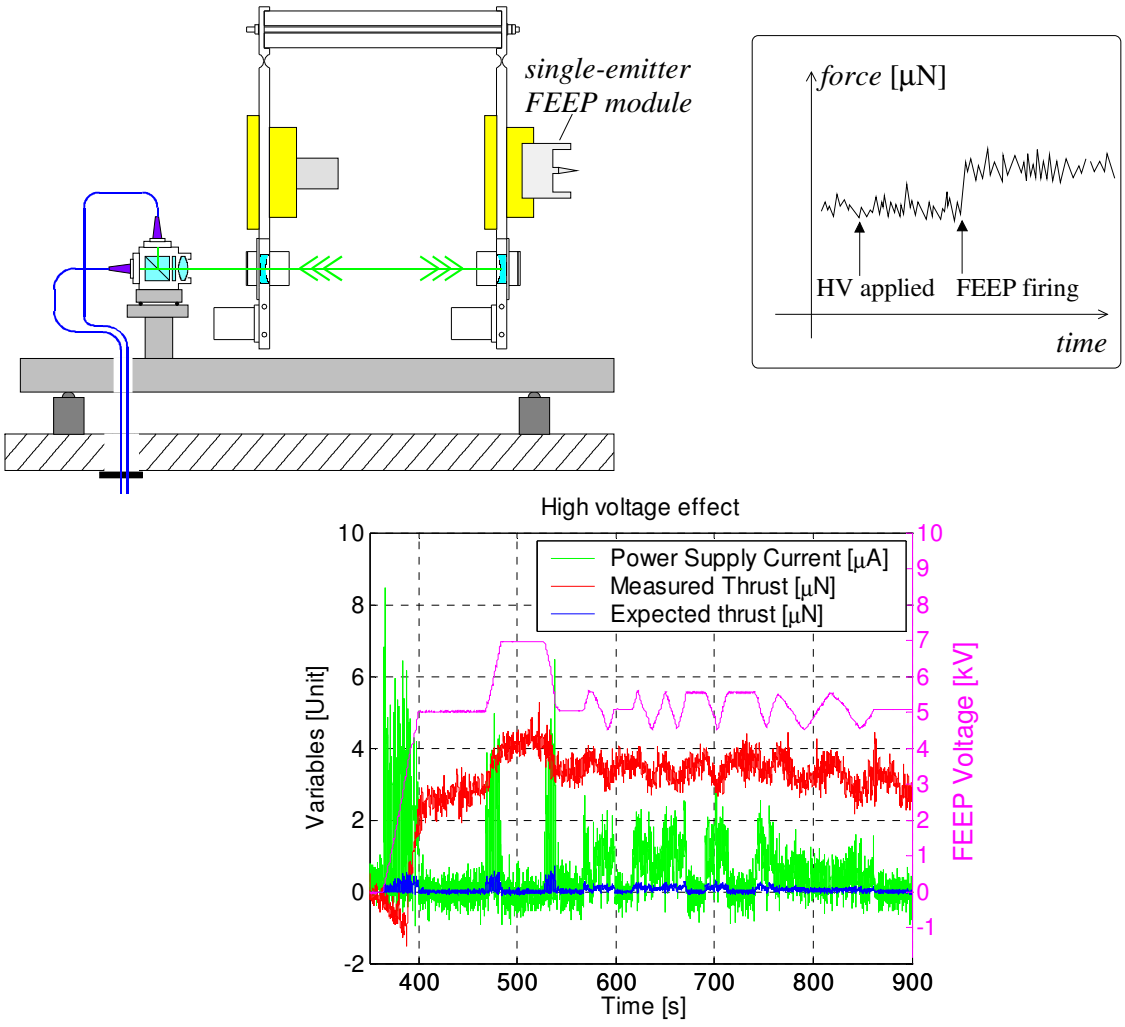

Figure 13, HV Effect on Force measurement (NB commissioning with SEM FEEP)

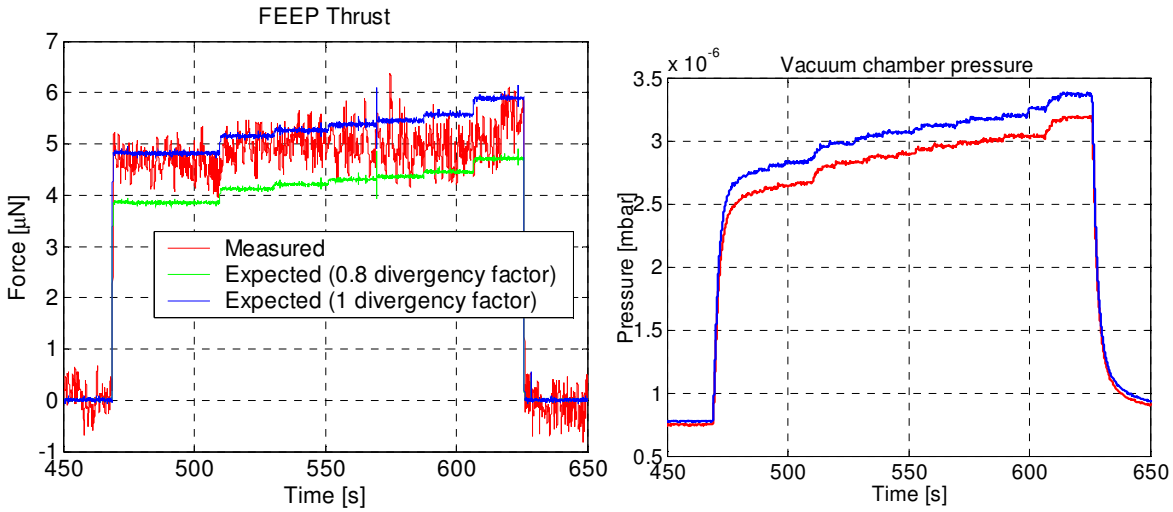

Figure 14, Thrust measurement test results: correlation vs different plume divergence simulations (NB commissioning with Indium-FEEP)

B. Cold Gas Thrusters

The main CGT typical causes of noise have been correlated, due to:

- pressurization and pressure variation inside the pipe routing (leakage, piping stiffness, piping deformation), Figure 15
- the effect of gas flow injected into the vacuum chamber (inflow), Figure 16
- Moving mass (piezo disk, plunger) inside the thruster valve, Figure 17

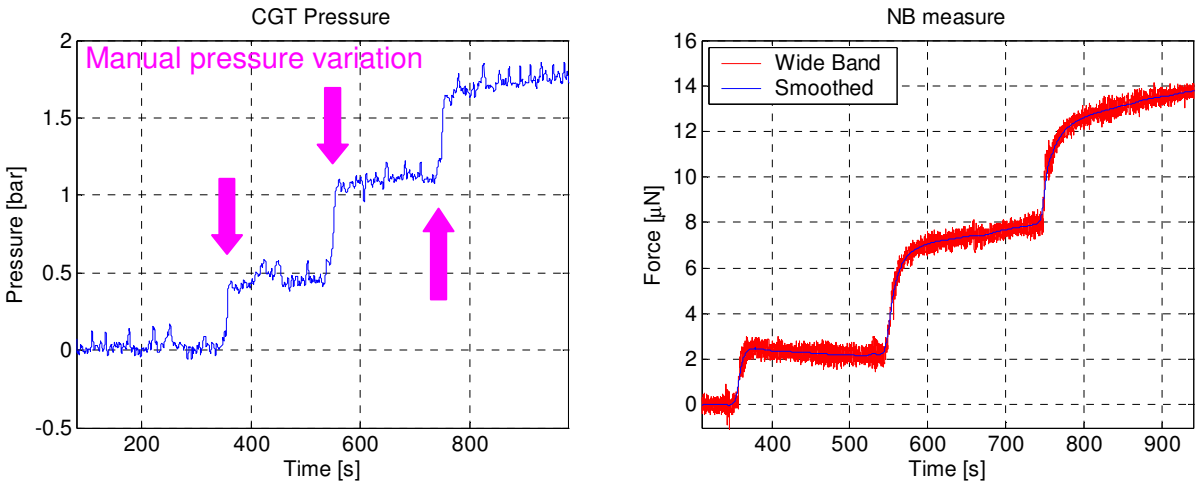

Figure 15, Measured force due to piping pressurization (NB commissioning with CGT)

The inflow effect is measured by mounting, thanks to a dedicated setup, the thruster in the same operative position but mechanically disconnected from the tilting plate, so that the thrust is not directly transmitted to the NB. The measured force is therefore due to inflow effect.
With the tested set-up the inflow parasitic effect has been found negligible up to a flow of 1 scc/min, 1 μN (conservative) from 1 to 10 scc/min, 20 μN from 10 to 100 scc/min.
This contribution is taken into account in the NB measurement accuracy definition.

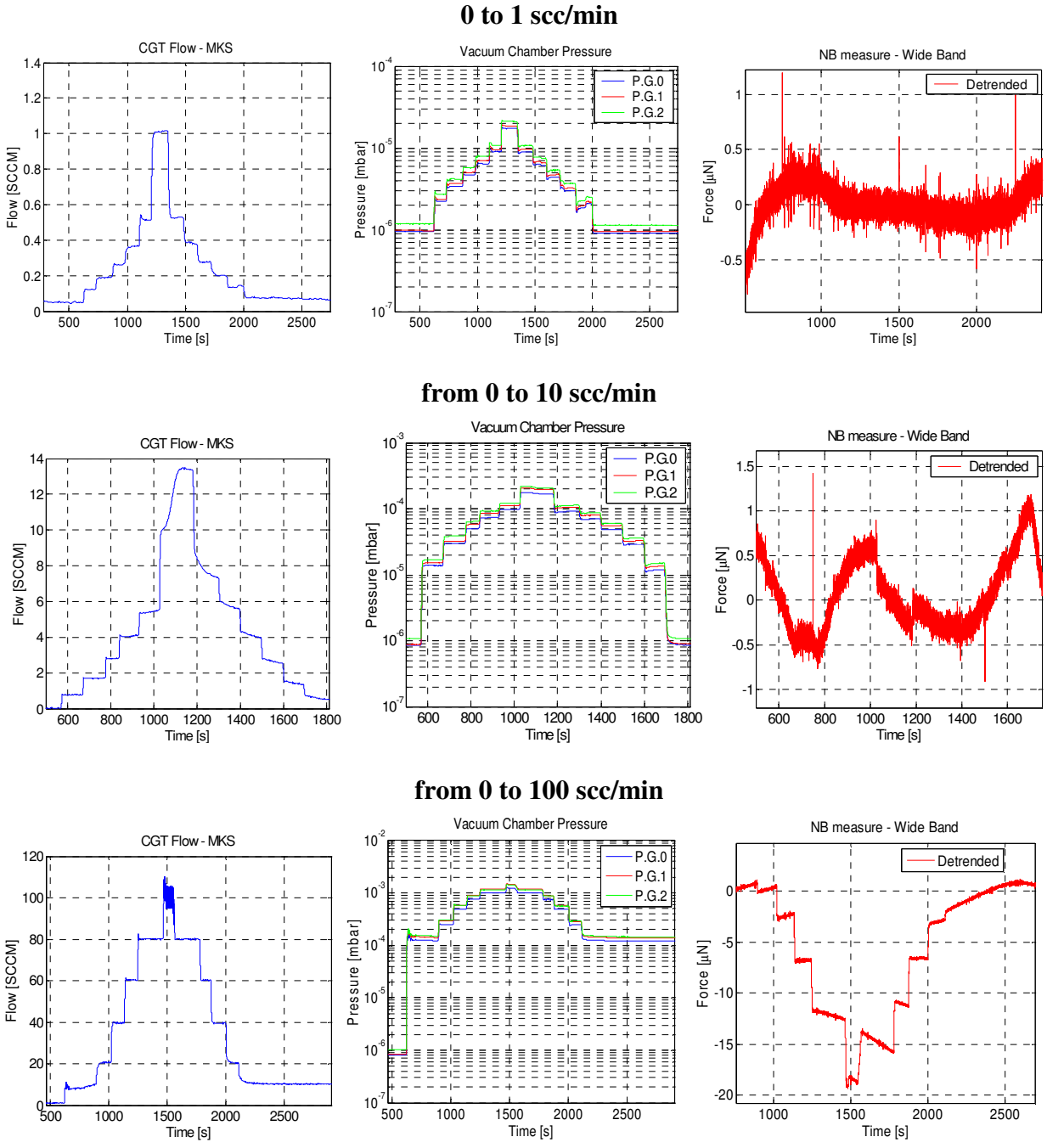

Figure 16, Measured force due to inflow effect under inject mass flow steps up to 100 scc/min (NB commissioning with CGT)

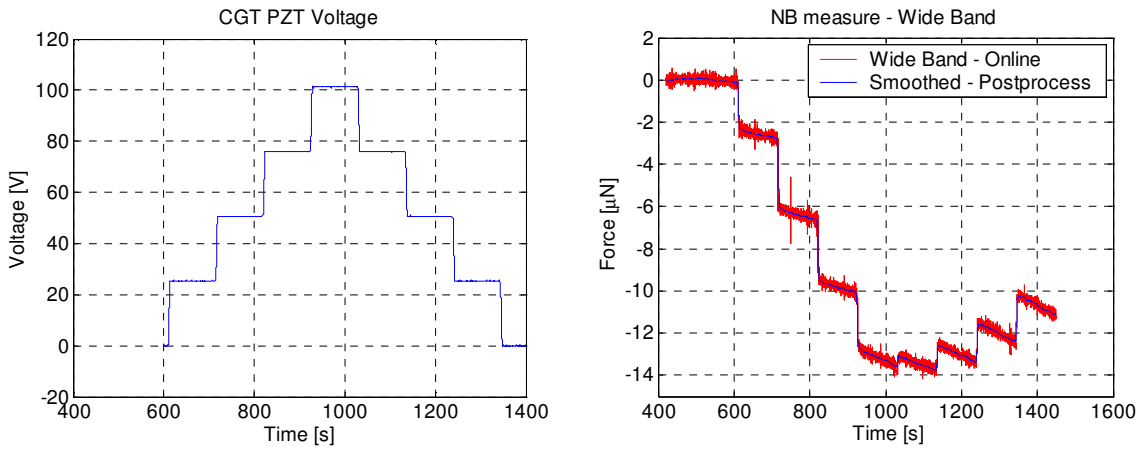

Figure 17, (Left): CGT applied voltage (Right): NB Measure)

Measured parasitic force due to the moving mass inside the CGT thruster valve can be partially modelled and removed with data post-processing, but can not be completely eliminated. Infact, if the CGT valve works with a piezoelectric actuator (PZT) moving the thruster plunger, the creep and hysteresis of the piezoelectric actuator introduce a model residual error (around 1÷ 2 μN) witch is checked and verified at the begin of the test campaign. NB measurement accuracy is so calculated considering also this contribution.

VIII. Conclusion

The Nanobalance Facility can fit, in the limit of the performances above illustrated, different typologies and sizes of thruster, having been thought as a multi-purpose facility. For this reason it can support the development of micro-propulsion for any space programmes needing this kind of actuation system.

It has been extensively commissioned through long test campaign before declaring it mature to operate.

At present the NB has already experienced other test campaigns for customers, carried out on both CGT and FEEP thrusters fed by Cesium. A further test campaign is planned in the next months for the characterization of Xenon-fed miniaturized Radiofrequency Ion Thrusters (RIT).

References

Eric D. Black
"An Introduction to Pound-Drever-Hall laser frequency stabilization"
Laser Interferometer Gravitational Wave Observatory – California Institute of Technology - Massachusetts Institute of Technology - Publication LIGO-P990042- A- D 04/04/00

John K. Ziemer
"Performance Measurements Using a Sub-Micronewton Resolution Thrust Stand"
Jet Propulsion Laboratory, M/S 125-109
California Institute of Technology - Published by the Electric Rocket Propulsion Society with permission.

Simone Rocca, University of Padova, Italy - and - Davide Nicolini, European Space Agency, Noordwijk, The Netherlands
"Micro-Thrust Balance Testing and Characterization"
Presented at the 29th International Electric Propulsion Conference, Princeton University, October 31 – November 4, 2005

Cesare S. et al.
"*The Nanobalance Facility",* in *Atelier Micro Propulsion Spatiale,* 2004. Toulouse, France.

F. Musso
"Embedded Model Control: application to space laser interferometry", PhD dissertation thesis

Merkowitz S.M. et al.
"*A μNewton thrust stand for LISA",* Class. Quantum Grav.

Denis Packan, Jean Bonnet and Simone Rocca
Thrust Measurements with the ONERA Micronewton Balance
Presented at the 30th International Electric Propulsion Conference, Florence, September 17-20, 2007

Enrico Canuto, Andrea Rolino
Nanobalance: An automated interferometric balance for micro-thrust measurement
ISA Transactions® Vol.43 (2004), pages 169–187

Enrico Canuto
Active vibration suppression in a suspended Fabry-Pérot cavity
ISA Transactions® Vol.45, Number 3, July 2006, pages 329–346

Enrico Canuto, Fabio Musso, and José Ospina,
Embedded Model Control: Submicroradian Horizontality of the Nanobalance Thrust-Stand
IEEE Transactions on Industrial Electronics, Vol.55, No.9, September 2008